

Estimating the effects of water-induced shallow landslides on soil erosion

Claudio Bosco¹ and Graham Sander¹

¹ Loughborough University, Department of Civil and Building Engineering
Loughborough, United Kingdom

This manuscript has been submitted to IEEE Earthzine.
It is still under peer review.

IEEE Earthzine 2014 Vol. 7 Issue 2, (still under review)
2nd quarter theme. Geospatial Semantic Array Programming

Abstract

Rainfall induced landslides and soil erosion are part of a complex system of multiple interacting processes, and both are capable of significantly affecting sediment budgets. This may potentially impact on a broad network of ecosystems, also altering the services they provide. To support the integrated assessment of these processes it is necessary to develop reliable modelling architectures. This paper proposes a semi-quantitative integrated methodology for a robust assessment of soil erosion rates in data poor regions affected by landslide activity. It combines heuristic, empirical and probabilistic approaches. This proposed methodology is based on the geospatial semantic array programming paradigm and has been implemented on a catchment scale methodology using GIS spatial analysis tools and GNU Octave. The integrated data-transformation model relies on a modular architecture, where the information flow among modules is constrained by semantic checks. In order to improve computational reproducibility, the geospatial data transformations implemented in ESRI ArcGis are made available in the free software GRASS GIS. The proposed modelling architecture is flexible enough for future transdisciplinary scenario-analysis to be more easily designed. In particular, the architecture might contribute as a novel component to simplify future integrated analyses of the potential interaction landslide/erosion by water to be performed not only for current land-cover but also exploring ecological disturbances such as wildfires and plant pest outbreaks.

1 Introduction

Hillslope processes can be envisaged as a cascade where surface erosion and mass movements are visible expressions of critical instabilities in a complex system of interacting processes that

15 control the downslope movement of material [1] in [2]. Field observations, modelling simulations
16 and experimental studies have shown that soil erosion can vary considerably due to the changes
17 in soil properties, vegetation cover and topography occurring after a landslide (e.g. [3, 4, 5]).
18 Following landslide events the changes in soil erosion rates can be strong enough to deliver
19 significant cascading impacts on ecosystems, for example due to an increased sediment yield
20 to a stream network. This may potentially be of ecological and economical relevance not only
21 locally (possibly driving complex changes even at the landscape-scale [6, 7]) but also off-site,
22 whenever ecosystem services are important for service benefit areas connected through service
23 connecting areas [8] (e.g. stream networks).

24 As natural resources are intrinsically entangled in complex networks there is a growing awareness
25 of the importance of these cascades. This, in turn is driving the development of integrated risk
26 assessment and multi-purpose use optimization of different resources to develop appropriate
27 management policies that can reliably model the potential influence of climate change on these
28 process cascades, and assess the resultant economic and societal consequences.

29 Landslide events will result in changes in topography and vegetation cover which in turn will
30 alter surface erosion rates and sediment yields. There are a number of relevant models that
31 use an integrated approach to soil erosion and landslide processes, including SHETRAN [9],
32 TOPOG [10, 11], PSIAC [12] or SIBERIA [13]. WEPP-SLIP (Water Erosion Prediction project
33 Shallow Landslide Integrated Prediction) [3] is a model that explicitly considers post-failure
34 sediment yield. This model integrates the physical basis of the WEPP model [14], with the
35 infinite slope stability model of Skempton and DeLory [15]. WEPP-SLIP is able to consider the
36 post-failure changes in soil erosion rate through the changes in topography and land cover.

37 Physically based models use a dynamic hydrological approach and local terrain characteristics
38 for estimating spatial and temporal landslide probability [16]. The main limits of physically
39 based models are that they are often optimised for small catchments and local conditions, and
40 that these require in depth knowledge of local soil and climatological parameters [17]. Empirical
41 methods are mainly based on the estimation of thresholds related to precipitation patterns which
42 result in landslide occurrence [16]. This approach generally requires high temporal resolution
43 rainfall data, which is not often available, and does not necessarily model the right processes.
44 In addition it is limited to being applicable to only the same conditions under which it was
45 developed [18, 17]. However, there is still room to improve the modelling of the interactions
46 of these processes, for example through assessments of the changes in surface area made more
47 susceptible to soil erosion following landslide events.

48 To quantify the potential changes in soil erosion due to landslide occurrence it is necessary to
49 know where and when on the slope a landslide initiates and how it evolves. This paper aims to
50 present a new modelling approach for data-poor regions in an attempt to improve the estimation
51 of sediment budgets derived from rainfall induced landsliding and soil erosion. A statistical
52 approach is proposed that is based on incorporating the frequency-area landslide distribution
53 model of Malamud et al. [19] within the framework of a spatially distributed empirical soil
54 erosion model.

55 2 the study area

56 The study area (Fig.1) is situated in southern Italy in the Daunia Appennines of the Puglia region,
57 within the municipal territory of Rocchetta Sant'Antonio. It covers an area of almost 10 km².
58 This area is highly susceptible to landslide activity [20, 21] with a consequent negative impact on
59 the local economy [22]. The area neighbouring to the north-west of the Rocchetta Sant'Antonio
60 territory presents a landslide frequency exceeding 20% for the overall area [23, 24, 22, 25]. Soil
61 erosion is also widespread and the severity is largely determined by the combination of tillage

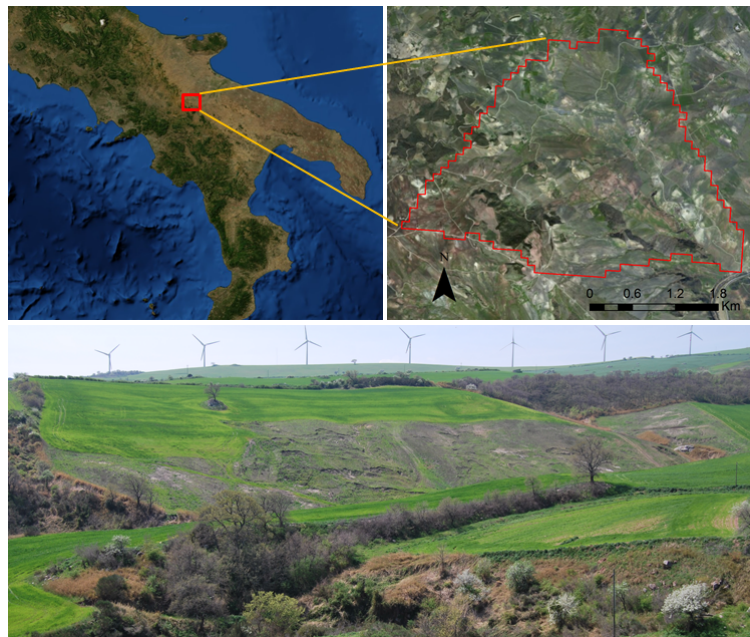


Figure 1: The study area (Rocchetta Sant'Antonio, Italy). Google Earth, ©2013 Google.

62 practices and the high erodibility of the clay-rich flysch units from which some of the local soils
63 are derived [26]. Within the catchment it is possible to distinguish four major classes of land use
64 (agricultural soils, woodland, pastures and grassland) and three dominant lithologies (limestone,
65 sandstone and clay). Slope angles are on average approximately 10 degrees with peak slope
66 angles rarely exceeding 25 to 30 degrees. An ephemeral drainage network is fed by precipitation
67 during the autumn-winter period when some 600 to 750 mm of rainfall is common [22]. The
68 area is characterized by a Mediterranean sub-humid climate.

69 **3 A new architecture for coupling of the effects of rainfall-** 70 **induced shallow landslides and soil erosion**

71 **3.1 geospatial semantic array programming**

72 Array programming is an approach for simplifying complex algorithm prototyping with an
73 accurate and compact mathematical description. It originates as a means for reducing the gap
74 between mathematical notation and its implementation within the model's algorithms in a
75 formalised and reproducible way. As stated by Iverson [27]: “the advantages of executability and
76 universality found in programming languages can be effectively combined, in a single coherent
77 language, with the advantages offered by mathematical notation”. Array programming has been
78 used for building the architecture for our modelling approach. For mitigating the complexity
79 of trans-disciplinary modelling and the inconsistencies between input data, parameters and
80 output, semantic checks on the processed information and a modularisation of the key parts
81 of the model were introduced following the semantic array programming paradigm (SemAP)
82 [28, 29, 30]. The proposed architecture (Fig. 2) exploits the geospatial capacities of Geographic
83 Information Systems (GIS) in order to estimate soil erosion yield (e-RUSLE model). In our
84 approach we integrated SemAP and geospatial tools (ArcGis and GRASS GIS) through the
85 Geospatial Semantic Array Programming paradigm (GeoSemAP). GeoSemAP exploits geospatial
86 tools and Semantic Array Programming for splitting a complex data-transformation-model

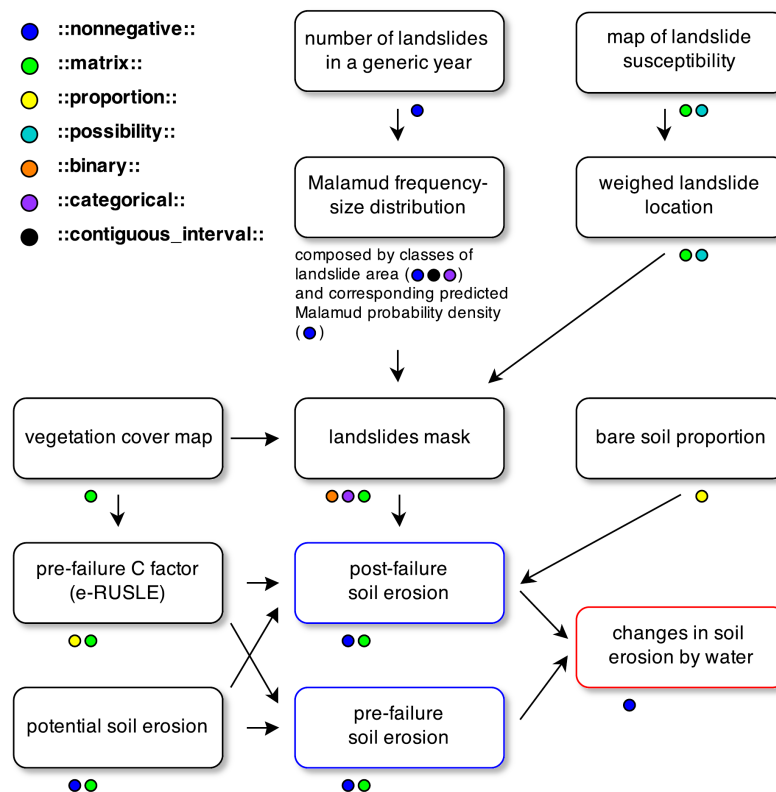


Figure 2: Flowchart of the model. The semantic aspects of the data-transformations among model components are highlighted within the workflow.

87 (D-TM) into logical blocks whose reliability can more easily be checked by applying geospatial
88 and mathematical constraints.

89 Semantic checks are exemplified in the following paragraphs with the notation **::constraint::**.
90 The semantic constraints were implemented within the code with a specialised module [31] of
91 the Mastrave modelling library. A hyperlink to the corresponding online description is provided.

92 3.2 applied techniques

93 The pre- and post-failure soil loss rate was calculated by applying the low data demanding
94 model e-RUSLE [32]. This model retains all the equations of its predecessor (RUSLE, [33]) and
95 implements an extra factor to account for the effects of soil stoniness on soil erosion. Due to the
96 flexibility of the modelling architecture that e-RUSLE is based on, it is possible to calibrate
97 the model for application at different scales [32]. e-RUSLE was implemented using the ArcGIS
98 software to first estimate the **::nonnegative::**¹ **::matrix::**² representing the soil erosion rates
99 within the catchment without considering the influence of mass movement. The scripts applied
100 for calculating the soil erosion losses can also be easily carried out using an Open Source Free
101 Software such as GRASS GIS or Quantum GIS.

¹http://mastrave.org/doc/mtv_m/check_is#SAP_nonnegative

²http://mastrave.org/doc/mtv_m/check_is#SAP_matrix

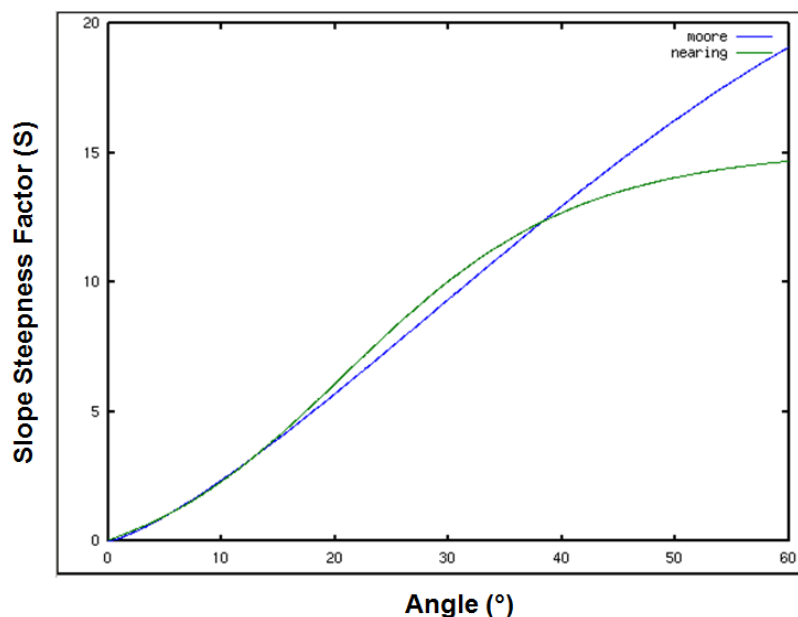


Figure 3: Comparison between the Moore and Burch [41] relation and the Nearing's [39] formula applied for calculating the S factor of the e-RUSLE model.

102 To determine the slope length factor required in e-RUSLE, the D-infinity (D_∞) algorithm of
 103 Tarboton [34] was first used to calculate the flow direction and then the flow length. Due to
 104 the geomorphological characteristics of the study area, a multiple-neighbour flow algorithm was
 105 required with the D_∞ algorithm being one of the most suitable [35, 36, 37]. In GRASS GIS it is
 106 possible to apply a multiple-flow approach using the tool 'r.watershed' [38]. The slope steepness
 107 factor was also slightly modified in comparison to the application of the e-RUSLE presented
 108 in Bosco et al. [32]. This was based on the Nearing's [39] equation which performs best for
 109 higher slopes [40, 32]. However the Moore and Burch [41] formula is more appropriate for slopes
 110 lower than 12.73 degrees because it gives the correct limiting value of zero in absence of any
 111 steepness. A comparison of both formulas is presented in Fig. 3, where a close matching trend
 112 is observed between 0 and 12.73 degrees (or 0 - 0.22 rad). Consequently a merged formula can
 113 be obtained by using the Moore and Burch equation for slopes less than 12.73 degrees and then
 114 the Nearing formula for higher slopes. To calculate the slope steepness factor of the model, the
 115 tool r.slope.aspect [42] of GRASS can be used. The majority of the equations that e-RUSLE is
 116 based up have been applied using the ArcGis tool 'Map Algebra' that in GRASS corresponds to
 117 'r.mapcalc' [43].

118 For quantifying the effect of size, position and number of landslides affecting this catchment the
 119 frequency-size distribution model proposed by Malamud et al. [19] was adopted. They found
 120 that landslide data from three quite different locations around the world (Italy, Guatemala and
 121 the USA) could be described quite well with the inverse gamma distribution

$$p(A_L, \rho, a, s) = \frac{1}{a\Gamma(\rho)} \left[\frac{a}{A_L - s} \right]^{\rho+1} \exp \left[-\frac{a}{A_L - s} \right] \quad (1)$$

122 In (1), p = probability density (km^{-2}), Γ is the gamma function, A_L = the landslide area (km^2),
 123 ρ (-) is a parameter which controls the power law decay for medium and large landslide areas, a
 124 (km^2) determines the position of the maximum in the probability distribution and s (km^2) is a
 125 parameter which fits the exponential decay behaviour for small landslide areas. Parameter values

126 of $\rho = 1.4$, $a = 1.28 \cdot 10^{-3} \text{ km}^2$ and $s = -1.32 \cdot 10^{-4} \text{ km}^2$ were shown to provide a good fit to the
127 measured data. A dataset of more than 400 reported landslides that affected the catchment
128 in 2006 was made available and published by Dr Janusz Wasowski of CNR-IRPI, Bari [22, 25].
129 For obtaining the landslide inventory, high resolution IKONOS satellite imagery was used. To
130 make the interpretation easier, the satellite images were orthorectified and pansharpened. This
131 dataset is not freely available but the IFFI database [44] is a valuable alternative to apply our
132 modelling approach whenever enough data are available.

133 Overall a reasonable correlation between the inverse-gamma distribution of Malamud et al. [19]
134 with the above parameter values and the frequency-size distribution of the landslide database
135 was found (Fig. 4). The fit is very good for landslide areas greater than or equal to the peak
136 in the distribution. For smaller landslide areas to the left of the peak the agreement is not
137 as good, though modifications to parameters a and s could be made to improve this section.
138 However the distribution of Malamud et al. [19] and parameter values they used, were shown
139 to work over a wide range of landslide sizes from various countries around the world. It was
140 found that these same parameter values also provided a similar fit to the data from our field
141 site suggesting the possibility of universality in the parameter values and therefore removing
142 the need for calibrating the distribution for local applications. On this basis we wanted to see
143 how well this would perform against data from the Rocchetta catchment and kept the original
144 Malamud parameter values. The data for the smaller landslides does have a greater degree of
145 uncertainty as its collection could easily have led to either an over or underestimation of the
146 landslide number. This could occur through either medium landslides being classified as smaller
147 due to being covered by larger landslides, or though the smaller landslides being covered by
148 larger ones and therefore missed completely. The main point of this exercise wasn't to match
149 exactly the landslide-area probability distribution, but to have a physically realistic distribution
150 on which to base our modelling. To predict when and where a landslide will occur is one of
151 the main challenges for calculating post-failure soil loss in data-poor regions. We exploited the
152 correlation between the measured data and Malamud's distribution through combination with
153 Monte Carlo simulation to analyse the effects of mass movements on soil erosion by water.

154 Assuming the validity of the proposed inverse-gamma function for calculating the probability
155 distribution of landslide areas we implemented a simple script (based on SemAP) in the
156 MATLAB language. Starting from a `::scalar_positive::`³ number to represent the number of
157 landslides that occurred in the catchment, we then calculate the number of landslides $\delta N_L(h)$
158 in the h -th class of landslides. Each class is a `::categorical_interval::`⁴ which includes all
159 the landslides with an area from $A_L(h)$ to $A_L(h + 1)$. The classes thus form a partition of
160 `::contiguous_interval::`⁵ s in $[0, A_L(hmax)]$ whose values are found from:

$$\delta N_L(h) = \int_{A_L(h)}^{A_L(h+1)} p(A_L) dA_L \quad (2)$$

161 In order to evaluate the effect of the post-failure changes on the soil erosion rates in the
162 catchment, we applied the Monte Carlo method twice. Once to randomly determine the location
163 of a landslide and a second time to sample the Malamud distribution to assign its size. The
164 Monte Carlo simulation was also implemented in the MATLAB language following the SemAP
165 paradigm and exploiting the potentiality offered by the Mastrave Library [29] whose tools were
166 largely used within the code.

³http://mastrave.org/doc/mtv_m/check_is#SAP_scalar_positive

⁴http://mastrave.org/doc/mtv_m/check_is#SAP_categorical-interval

⁵http://mastrave.org/doc/mtv_m/check_is#SAP_contiguous_interval

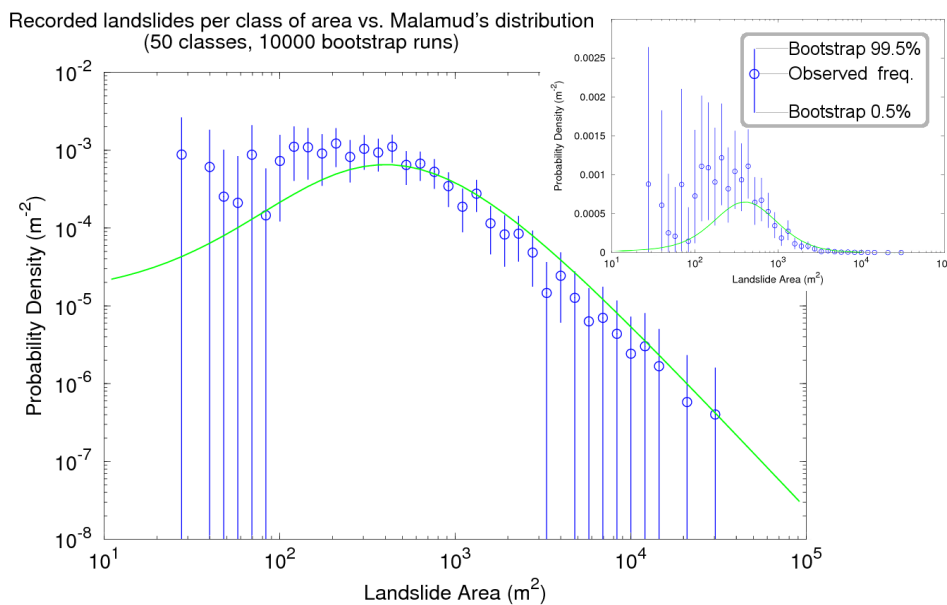


Figure 4: Dependence of the landslide probability densities on landslide area for the measured set of data (blue) and for Malamud's distribution (green). The probability density is given on logarithmic and semi-logarithmic scale. A bootstrap analysis was performed for assessing the uncertainty of the measured data.

167 To be more explicit: considering Y as a random variable distributed according to a given
 168 probability distribution, it is possible to generate n pseudo-random instances Y_1, \dots, Y_n with the
 169 same distribution. This may be accomplished with a classical Monte Carlo extraction. Let us
 170 define $f(\cdot)$ as a certain function of Y which is implemented, within the SemAP paradigm, as a
 171 D-TM transforming an instance of Y into the desired output data. Suppose we are interested in
 172 computing the integral A of $f(\cdot)$ over a given domain. This implies considering the probability
 173 density function $\pi(\cdot)$ of Y over :

$$\begin{aligned}
 & Y \in \Omega \\
 & Y \sim \Phi \\
 & A = \int_{\Omega} f(Y) \cdot \pi(Y) dY, \quad \pi(Y) \text{ density function of } \Phi \text{ in } Y \\
 & \text{such that } \int_{\Omega} \pi(Y) dY = 1
 \end{aligned} \tag{3}$$

174 Numerically, it is possible to approximately estimate A by exploiting the n Monte Carlo instances
 175 Y_1, \dots, Y_n as

$$A \approx \hat{A}_n = \frac{1}{n} \sum_{\text{run}=1}^n f(Y_{\text{run}}), \quad \forall \text{run}, Y_{\text{run}} \sim \Phi \tag{4}$$

176 where Y_{run} is the run -th instance of Y corresponding to the run -th Monte Carlo iteration. From
 177 the law of large numbers, if $n \Rightarrow \infty$, $\hat{A}_n \Rightarrow A$. In our particular application, \hat{A}_n is the average
 178 over n runs of simulated landslides; in each of them the total erosion by water $f(\cdot)$ is computed
 179 for the particular array of landslides Y_{run} . The n arrays of simulated landslides are the basis for
 180 $f(\cdot)$ to estimate the corresponding post-landslide soil erosion. Each landslide occurring in the

181 *run*-th simulation has an area distributed according to $\bar{p}(\cdot)$. This defines $\pi(\cdot)$ as the probability
182 density function with which each *run*-th array of landslides is distributed.

183 The Monte Carlo simulation was iterated 1000 times. For each of the iterations the post-failure
184 changes in soil erosion were calculated and compared with the pre-failure estimates.

185 The [::matrix::](http://mastrave.org/doc/mtv_m/check_is#SAP_matrix)⁶ representing the cover management factor of the e-RUSLE model was calculated
186 using a 5x5 metres resolution land cover map of the study site, produced by CNR-IRPI of
187 Bari using ASTER satellite multi-spectral imagery and published in [22]. The map is not
188 freely available but the CLC [45] is a valid open access alternative. The post-failure changes in
189 vegetation cover were used within the model for estimating the effect of mass movement on soil
190 erosion. Because of the modular modelling architecture (Fig. 2), the module that calculates the
191 pre-failure C factor can be used as a link among our model and other approaches for measuring
192 different land disturbance effects, in order to measure their effects on soil erosion.

193 The post-failure vegetation cover results were only partially altered by the slow mass movements
194 that characterize this catchment (see fig. 1). As locally the slide surface may also remain
195 unchanged, we introduced into the model a value representing the post-failure percentage of bare
196 soil. By analysing the landslide dataset, the available pictures, satellite images and accounting
197 for all the information collected during a field survey carried out within the study area, the
198 percentage of the post-failure bare soil cover was estimated to be not less than 20% of the
199 landslide area. For each of the pixels of the modelled landslides in each of the 1000 Monte
200 Carlo iterations, the [::scalar_positive::](http://mastrave.org/doc/mtv_m/check_is#SAP_scalar_positive)⁷ [::proportion::](http://mastrave.org/doc/mtv_m/check_is#SAP_proportion)⁸ of bare soil was therefore randomly
201 determined in the range 0.2 - 1.

202 4 Results and discussion

203 Table 1 shows the results of the Monte Carlo simulations. We replaced the mean values obtained
204 by applying equation 4, with the median, because it is more stable in that it is only marginally
205 affected by extreme values. By analysing the median on 1000 simulations of the cumulated
206 pre-failure and post-failure soil erosion, an increase of 20% of the total soil loss was estimated.
207 The post-failure soil erosion rate in areas where landslides occurred is, on average, around 3.5
208 times the pre-failure value.

209 A bootstrap analysis, based on 10,000 runs, was performed for assessing uncertainty. The
210 analysis of the changes in the rate of soil erosion due to landslide occurrence shows post-failure
211 increases in soil loss of approximately 1700 tons per year (bootstrap $p \leq 0.05$). This corresponds
212 to an increase of around 22% of the total soil erosion. We also analysed the extension of the
213 area affected by slope instability. The bootstrap analysis shows that in each simulation at least
214 76 hectares, corresponding to around 8.5% of the catchment, is affected by landslide activity
215 (bootstrap $p \leq 0.05$). By comparing this value with the area that presented slope instability
216 in 2006 (around 55 hectares), the applied methodology seems to slightly overestimate. The
217 graph in figure 3 shows that Malamud's distribution seems to underestimate the number of
218 small landslides ($< 300 m^2$). Nevertheless, the probability density distribution for the Rocchetta
219 landslides from 2006 is in line with those reported by Malamud et al. [19] for precipitation
220 triggered landslides that took place in Guatemala in 1998. The model is in its early developmental
221 phase and fine tuning the fit of the Malamud distribution to small landslides should help to
222 improve the model predictions. However, for better evaluating the limits or the robustness of the
223 proposed inverse-gamma distribution or of a modified version, further data would be necessary.
224 The bootstrap analysis, with 10000 runs, performed on the measured data (Fig. 4) shows the

⁶http://mastrave.org/doc/mtv_m/check_is#SAP_matrix

⁷http://mastrave.org/doc/mtv_m/check_is#SAP_scalar_positive

⁸http://mastrave.org/doc/mtv_m/check_is#SAP_proportion

Table 1: Bootstrap analysis of the modelling results. The bootstrap analysis, based on 10000 runs, shows the bootstrap cumulated distribution of the pre-and post-failure soil erosion within the area affected by landslide activity.

Quantile	Pre-failure soil loss (t)	Post-failure soil loss (t)	Estimated landslide activity area (ha)
5%	744.7	2530.3	76.6 (8.4%)
25%	799.2	2762.3	84.4 (9.2%)
50%	828.7	2773.3	85.5 (9.4%)
75%	843.4	2896	87.1 (9.6%)
95%	854.6	3005	88.9 (9.8%)

225 uncertainty associated with a single year landslide dataset is too high for extrapolating different
226 parameter values. A more detailed analysis based on datasets covering a longer time interval
227 would help in improving the applied methodology. An additional source of error contributing
228 to the predictions that needs further investigation, arises from the selection of the model for
229 estimating soil erosion and its running with limited data, thus there is considerable scope for
230 errors in prediction to be strongly linked to this simplification.

231 Because the capacity to estimate the changes in soil erosion from landslide activity is largely
232 dependent on the quality of the available datasets, the applied methodology broadens the
233 possibility of a quantitative assessment of these effects in data-poor regions. The obtained
234 results, even considering a possible overestimation, confirm the important role of mass movements
235 on soil erosion and the consequent necessity to better integrate these processes into soil erosion
236 modelling.

237 5 Conclusions

238 A new method for empirically estimating the importance and extent of landslides on soil
239 erosion losses in data-poor regions has been developed. This has been achieved by sampling
240 the frequency-size landslide distribution proposed by Malamud et al. [19], and stochastically
241 distributing the landslide location across the catchment. Given the increasing threat of soil
242 erosion all over the world and the implications this has on future food security and soil and water
243 quality, an in-depth understanding of the rate and extent of soil erosion processes is crucial.

244 Each year, on average, between 8.5 and 10% of the catchment shows evidence of landslide
245 activity that is responsible for a mean increase in the total soil erosion rate between 22 and 26%
246 over the pre-failure estimate. These results confirm the potential importance of integrating the
247 landslide contribution into soil erosion modelling. While this approach clearly has limitations
248 the proposed approach can be seen as a first attempt to assess the landslide-erosion interaction
249 in areas with limited data.

250 The proposed modelling approach is also suitable to be applied in applications having a wider
251 spatial extent and to be potentially implemented in a transdisciplinary context. For example, the
252 relevant effect of wildfires on soil erosion and landslide susceptibility [46, 47] could be modelled
253 with a higher reliability integrating the proposed approach. As stated in de Rigo et al. [47],
254 wildfires can considerably increase soil erosion by water and landslide susceptibility. The changes
255 in landslide susceptibility may in turn affect soil erosion. In general, considering the modelling

256 architecture (Fig. 2), if the module that calculates the pre-failure C factor value would provide
257 the layer altered by a different disturbance (e.g. wildfires or pests outbreak), the presented
258 modelling architecture could be applied for estimating the indirect effect of these disturbances
259 on soil erosion, provided a new landslide susceptibility map, that considers the altered vegetation
260 cover, is produced .

261 Although the preliminary results are promising, further research is required before this method
262 can be applied by the scientific community and relevant authorities with any level of confidence.
263 Consideration of, and integrating within the model, post-failure changes in topography and soil
264 characteristics (e.g. soil armouring [48]) is fundamental for increasing the predictive capacity of
265 the model. Also a better estimation of the bare soil exposed within a landslide is fundamental for
266 improving our model. It would also be worthwhile to improve the fit of the Malamud distribution
267 to the data that, at the present, it is not possible due to the limited availability of measured
268 data. For obtaining more reliable results, and more robust estimates of the effects of landslides
269 on soil and vegetation cover, it will be also necessary to focus attention on producing a less
270 uncertain zonation of the spatial probability of the landslide susceptibility in areas characterized
271 by low data availability [49].

272 Acknowledgements

273 We would like to thank Dr. Tom Dijkstra for his valuable comments on the manuscript. We
274 also would like to thank Dr. Janusz Wasowski and Dr. Caterina Lamanna for providing the
275 landslide data and Dr. Wasowski also for his fundamental support during fieldwork. This paper
276 is published with the support of the Maieutike Research Initiative.

277 References

- 278 [1] Th.W.J. van Asch, “Water erosion on slopes and landsliding in a Mediterranean landscape,”
279 Ph.D dissertation, Utrecht Univ., 1980.
- 280 [2] L.P.H. Van Beek, “Assessment of the Influence of Changes in Landuse and Climate on
281 Landslide Activity in a Mediterranean Environment,” Ph.D dissertation, Utrecht Univ.,
282 Utrecht, 2002.
- 283 [3] T.A. Cochrane, and Acharya, G., “Changes in sediment delivery from hillslopes affected by
284 shallow landslides and soil armouring,” *Journal of Hydrology (New Zealand)*, vol. 50, no. 1,
285 pp. 5-18, 2011.
- 286 [4] G. Acharya, T.A. Cochrane, T. Davies, E. Bowman, “The influence of shallow landslides on
287 sediment supply: A flume-based investigation using sandy soil,” *Engineering Geology*, vol.
288 109, pp. 161-169, 2009. doi: [10.1016/j.enggeo.2009.06.008](https://doi.org/10.1016/j.enggeo.2009.06.008) .
- 289 [5] G. Acharya, T. Cochrane, T. Davies, and E. Bowman, “Quantifying and modeling post-failure
290 sediment yields from laboratory-scale soil erosion and shallow landslide experiments with silty
291 loess,” *Geomorphology*, vol. 129, no. 1-2, pp. 49–58, 2011. doi: [10.1016/j.geomorph.2011.01.012](https://doi.org/10.1016/j.geomorph.2011.01.012) .
- 292 [6] M.M. Bakker, G. Govers, C. Kosmas, V. Vanacker, K. Oost, and M. Rounsevell, “Soil erosion
293 as a driver of land-use change,” *Agriculture, Ecosystems & Environment*, vol. 105, no. 3, pp.
294 467-481, 2005. doi: [10.1016/j.agee.2004.07.009](https://doi.org/10.1016/j.agee.2004.07.009) .
- 295 [7] M. Geertsema and J.J. Pojar, “Influence of landslides on biophysical diversity - a
296 perspective from british columbia,” *Geomorphology*, vol. 89, no. 1-2, pp. 55-69, 2007.
297 doi: [10.1016/j.geomorph.2006.07.019](https://doi.org/10.1016/j.geomorph.2006.07.019) .

- 298 [8] R.-U. Syrbe and U. Walz, “Spatial indicators for the assessment of ecosystem services:
299 Providing, benefiting and connecting areas and landscape metrics,” *Ecological Indicators*, vol.
300 21, pp. 80-88, 2012. doi: 10.1016/j.ecolind.2012.02.013 .
- 301 [9] J. Ewen, G. Parkin, P.E. OConnell, “SHETRAN: Distributed River Basin Flow and Transport
302 Modeling System,” *Journal of Hydrologic Engineering*, vol. 5, no. 3, pp. 250–258, 2000.
303 doi: 10.1061/(ASCE)1084-0699(2000)5:3(250) .
- 304 [10] E.M. O’Loughlin, “Prediction of surface saturation zones in natural catchments
305 by topographic analysis,” *Water Resour. Res.*, vol. 22, no. 5, pp. 794–804, 1986.
306 doi: 10.1029/WR022i005p00794 .
- 307 [11] CSIRO. (2010). *TOPOG Home page*. [Online]. Available: [http://www.per.clw.csiro.au](http://www.per.clw.csiro.au/topog/intro/intro.html)
308 [/topog/intro/intro.html](http://www.per.clw.csiro.au/topog/intro/intro.html) (archived at: <http://www.webcitation.org/6UNGXls01>)
- 309 [12] Pacific Southwest Inter-Agency Committee, “Report of the water management subcommittee
310 on factors affecting sediment yield in the Pacific southwest area and selection and evaluation
311 of measures for reduction of erosion and sediment yield,” 1968.
- 312 [13] G. Willgoose, and S.R. Riley, “Application of a catchment evolution model to the pre-
313 diction of long-term erosion on the spoil heap at Ranger uranium mine: Initial anal-
314 ysis,” Supervising Scientist Report, 132, Supervising Scientist, Canberra, 1998. [On-
315 line]. Available: [http://www.environment.gov.au/resource/application-catchment-e](http://www.environment.gov.au/resource/application-catchment-evolution-model-production-long-term-erosion-spoil-heap-ranger)
316 [volution-model-production-long-term-erosion-spoil-heap-ranger](http://www.environment.gov.au/resource/application-catchment-evolution-model-production-long-term-erosion-spoil-heap-ranger) (archived at: [ht](http://www.webcitation.org/6UNHHqe0k)
317 [tp://www.webcitation.org/6UNHHqe0k](http://www.webcitation.org/6UNHHqe0k)).
- 318 [14] J.M. Lafen, L.J. Lane, G.R. Foster, “WEPP: A new generation of erosion prediction
319 technology,” *Journal of Soil and Water Conservation*, vol. 46, pp. 34–38, 1991.
- 320 [15] A.W. Skempton, and F.A. DeLory, “Stability of natural slopes in London clay,” *ASCE*
321 *Journal*, vol. 2, pp. 378–381, 1957.
- 322 [16] P. Jaiswal, and C.J. van Westen, “Estimating temporal probability for landslide initiation
323 along transportation routes based on rainfall thresholds,” *Geomorphology*, vol. 112, pp. 96-105,
324 2009. doi: 10.1016/j.geomorph.2009.05.008 .
- 325 [17] J. de Vente, J. Poesen, G. Verstraeten, G. Govers, M. Vanmaercke, A. Van Rompaey,
326 M. Arabkhedri, and C. Boix-Fayos, “Predicting soil erosion and sediment yield at
327 regional scales: Where do we stand?,” *Earth-Sci. Rev.*, vol. 127, pp. 16–29, 2013.
328 doi: 10.1016/j.earscirev.2013.08.014 .
- 329 [18] R. Hessel, “Modelling soil erosion in a small catchment on the Chinese Loess Plateau,”
330 Ph.D. dissertation, Utrecht Univ., Netherlands, 307 pp., 2002.
- 331 [19] B.D. Malamud, D.L. Turcotte, F. Guzzetti, and P. Reichenbach, “Landslide inventories
332 and their statistical properties,” *Earth Surface Processes and Landforms*, vol. 29, no. 6, pp.
333 687-711, 2004. doi: 10.1002/esp.1064 .
- 334 [20] G. Iovine, M. Parise, E. Crescenzi, “Analisi della franosità nel settore centrale
335 dell’Appennino Dauno,” *Memorie della società Geologica Italiana*, vol. 51, pp. 633-641,
336 1996.
- 337 [21] P. Magliulo, A. Di Lisio, F. Russo, and A. Zelano, “Geomorphology and landslide suscepti-
338 bility assessment using GIS and bivariate statistics: A case study in southern Italy,” *Natural*
339 *Hazards*, vol. 47, no. 3, pp. 411-435, 2008. doi: 10.1007/s11069-008-9230-x .

- 340 [22] J. Wasowski, C. Lamanna, and D. Casarano, “Influence of land-use change and precipita-
341 tion patterns on landslide activity in the Daunia Appennines, Italy,” *Quarterly Journal of*
342 *Engineering Geology and Hydrogeology*, vol. 43, no. 4, pp. 387-401, 2010. doi: [10.1144/1470-](https://doi.org/10.1144/1470-9236/08-101)
343 [9236/08-101](https://doi.org/10.1144/1470-9236/08-101).
- 344 [23] Mossa S., Capolongo D., Pennetta L., Wasowski J., “A GIS-based assessment of landsliding
345 in the Daunia Apennines, southern Italy,” in *Proceedings of the International Conference*
346 *‘Mass Movement Hazard in Various Environments’*, M. Graniczny, M. Czarnogorska, et al.,
347 Eds. Warsaw, Poland: Polish Geological Institute, 2005, pp. 86–91.
- 348 [24] J. Wasowski, D. Casarano, and C. Lamanna, “Is the current landslide activity in the Daunia
349 region (Italy) controlled by climate or land use change,” in *Proceedings of the International*
350 *Conference on Landslides and Climate Change*, R. McInnes, J. Jakeways, H. Fairbank, E.
351 Mathie, Eds. London, UK: Taylor & Francis, 2007, pp. 41–49.
- 352 [25] J. Wasowski, C. Lamanna, G. Gigante, and D. Casarano, “High resolution satellite imagery
353 analysis for inferring surface-subsurface water relationship in unstable slopes,” *Remote sensing*
354 *of Environment*, vol. 124, pp. 135–148, 2012.
- 355 [26] C. Lamanna, D. Casarano, G. Gigante, and J. Wasowski, “Mappatura e studio dei fenomeni
356 franosi nel Subappennino dauno con immagini satellitari ad alta risoluzione,” in *Proc. 13a*
357 *conferenza Nazionale ASITA*, Bari, 2009.
- 358 [27] K.E. Iverson, “Notation as a tool of thought,” *Commun. ACM*, vol. 23, pp. 444–465, 1980.
359 doi: [10.1145/358896.358899](https://doi.org/10.1145/358896.358899).
- 360 [28] D. de Rigo, P. Corti, G. Caudullo, D. McInerney, M. Di Leo, and J. San-Miguel-Ayanz,
361 “Toward open science at the European scale: Geospatial Semantic Array Programming
362 for integrated environmental modelling,” *Geophys. Res. Abstr.*, vol. 15, 13245+, 2013.
363 doi: [10.6084/m9.figshare.155703](https://doi.org/10.6084/m9.figshare.155703).
- 364 [29] D. de Rigo, “Semantic array programming for environmental modelling: Application of the
365 Mastrave library,” in *International Environmental Modelling and Software Society (iEMSs)*
366 *2012 International Congress on Environmental Modelling and Software. Managing Resources*
367 *of a Limited Planet: Pathways and Visions under Uncertainty, Sixth Biennial Meeting*,
368 R. Seppelt, A.A. Voinov, S. Lange, and D. Bankamp, Eds., 2012, pp. 1167-1176. [Online].
369 Available: http://mastrave.org/bib/de_Rigo_iEMSs2012.pdf.
- 370 [30] D. de Rigo, *Semantic Array Programming with Mastrave - Introduction to Semantic*
371 *Computational Modelling*, The Mastrave Project, 2012. [Online]. Available: [http://mastra-](http://mastrave.org/doc/MTV-1.012-1/)
372 [ve.org/doc/MTV-1.012-1/](http://mastrave.org/doc/MTV-1.012-1/).
- 373 [31] D. de Rigo, “Applying semantic constraints to array programming: the module ”check_
374 is” of the Mastrave modelling library,” in: *Semantic Array Programming with Mastrave -*
375 *Introduction to Semantic Computational Modelling*, 2012. Available: [http://mastrave.org](http://mastrave.org/doc/mtv_m/check_is)
376 [/doc/mtv_m/check_is](http://mastrave.org/doc/mtv_m/check_is).
- 377 [32] C. Bosco, D. de Rigo, J. Poesen, O. Dewitte, and P. Panagos, “Modelling Soil Erosion at
378 European Scale: Towards Harmonization and Reproducibility,” *Nat. Hazards Earth Syst. Sci.*
379 *Discuss*, vol. 2, pp. 2639–2680, 2014. doi: [doi:10.5194/nhessd-2-2639-2014](https://doi.org/10.5194/nhessd-2-2639-2014).
- 380 [33] K.G. Renard, G.R. Foster, G.A. Weesies, D.K. McCool, and D.C. Yoder, “Predicting Soil
381 Erosion by Water: A Guide to Conservation Planning with the Revised Universal Soil Loss
382 Equation (RUSLE),” *USDA Agr. Handb.*, no. 703, 1997.
- 383 [34] D.G. Tarboton, “A new method for the determination of flow directions and upslope areas
384 in grid digital elevation models,” *Water Resources Research*, vol.33, no.2, pp. 309–319, 1997.

- 385 [35] S. Gruber, and S. Peckham, “Land-Surface Parameters and Objects in Hydrology” in *Geo-*
386 *morphometry: Concepts, Software, Applications*, T. Hengl and H.I. Reuter, Eds., Developments
387 in Soil Science, Elsevier, vol.33, 2009, pp. 171-194. doi: [10.1016/S0166-2481\(08\)00007-X](https://doi.org/10.1016/S0166-2481(08)00007-X).
- 388 [36] G.B. Chirico, A.W. Western, R.B. Grayson, and G. Bloschl, “On the definition of the
389 flow width for calculating specific catchment area patterns from gridded elevation data,”
390 *Hydrol.Process.*, vol. 19, pp. 2539-2556, 2005. doi: [10.1002/hyp.5730](https://doi.org/10.1002/hyp.5730).
- 391 [37] R.H. Erskine, T.R. Green, J.A. Ramirez, L.H. MacDonald, “Comparison of grid-based
392 algorithms for computing upslope contributing area,” *Water Resour. Res.*, vol. 42, W09416,
393 2006. doi: [10.1029/2005WR00464](https://doi.org/10.1029/2005WR00464).
- 394 [38] C. Ehlschlaeger, “GRASS GIS manual: r.watershed,” in: *GRASS Development Team, 2014.*
395 *GRASS GIS 7.0.0svn Reference Manual*. Open Source Geospatial Foundation, 2006. [Online].
396 Available: <http://grass.osgeo.org/grass65/manuals/r.watershed.html>.
- 397 [39] M.A. Nearing, “A single, continuous function for slope steepness influence on soil loss,” *Soil*
398 *Science Society of America Journal*, vol. 61, no. 3, pp. 917-919, 1997. [Online]. Available:
399 <http://handle.nal.usda.gov/10113/6603>.
- 400 [40] C. Bosco, E. Rusco, L. Montanarella, and S. Oliveri, “Soil erosion risk assessment in the
401 alpine area according to the IPCC scenarios,” in *Threats to Soil Quality in Europe*, G. Toth,
402 L. Montanarella, and E. Rusco, Eds., EUR 23438 EN, pp. 47–58, 2008.
- 403 [41] I. Moore, and G. Burch, “Physical basis of the length-slope factor in the universal soil
404 loss equation,” *Soil Science Society of America Journal*, vol. 50, no. 5, pp. 1294-1298, 1986.
405 doi: [0.2136/sssaj1986.03615995005000050042x](https://doi.org/0.2136/sssaj1986.03615995005000050042x).
- 406 [42] M. Shapiro, and O. Waupotitsch, “GRASS GIS manual: r.slope.aspect,” in: *GRASS*
407 *Development Team, 2014. GRASS GIS 7.0.0svn Reference Manual*. Open Source Geospatial
408 Foundation, 2006. [Online]. Available: [http://grass.osgeo.org/grass65/manuals/r.slope](http://grass.osgeo.org/grass65/manuals/r.slope.aspect.html)
409 [e.aspect.html](http://grass.osgeo.org/grass65/manuals/r.slope.aspect.html).
- 410 [43] M. Shapiro, and G. Clements, “GRASS GIS manual: r.mapcalc,” in: *GRASS Development*
411 *Team, 2014. GRASS GIS 7.0.0svn Reference Manual*. Open Source Geospatial Foundation,
412 2006. [Online]. Available: <http://grass.osgeo.org/grass64/manuals/r.mapcalc.html>.
- 413 [44] V. Agnesi, L. Arziello, P. Aucelli, A. Baglioni, C. Bettucci, et al., “Rapporto sulle frane in
414 Italia. Il Progetto IFFI - Metodologia, risultati e rapporti regionali, APAT, Rapporti 782007,”
415 p. 681, 2007. [Online]. Available: [http://www.progettoiffi.isprambiente.it/cartaneti](http://www.progettoiffi.isprambiente.it/cartanetiffi/carto3.asp?cat=40&lang=IT#)
416 [ffi/carto3.asp?cat=40&lang=IT#](http://www.progettoiffi.isprambiente.it/cartanetiffi/carto3.asp?cat=40&lang=IT#)
- 417 [45] European Environment Agency, “Corine Land Cover 2006 raster data - version 15 (08/2011),”
418 2011. [Online]. Available: [http://www.eea.europa.eu/data-and-maps/data/corine-land](http://www.eea.europa.eu/data-and-maps/data/corine-land-cover-2006-raster-1)
419 [d-cover-2006-raster-1](http://www.eea.europa.eu/data-and-maps/data/corine-land-cover-2006-raster-1).
- 420 [46] M. Di Leo, D. de Rigo, D. Rodriguez-Aseretto, C. Bosco, T. Petroliaqkis, A. Camia, and J.
421 San-Miguel-Ayanz, “Dynamic data driven ensemble for wildfire behaviour assessment: A case
422 study,” *IFIP Adv. Inf. Commun. Technol.*, vol. 413, pp. 11-22, 2013. doi: [10.1007/978-3-642-](https://doi.org/10.1007/978-3-642-41151-9_2)
423 [41151-9_2](https://doi.org/10.1007/978-3-642-41151-9_2).
- 424 [47] D. de Rigo, D. Rodriguez-Aseretto, C. Bosco, M. Di Leo, and J. San-Miguel-Ayanz, “An
425 architecture for adaptive robust modelling of wildfire behaviour under deep uncertainty,” *IFIP*
426 *Adv. Inf. Commun. Technol.*, vol. 413, pp. 367-380, 2013. doi: [10.1007/978-3-642-41151-9_35](https://doi.org/10.1007/978-3-642-41151-9_35).

- 427 [48] G. Acharya, and T.A. Cochrane, “Rainfall induced shallow landslides on sandy soil and
428 impacts on sediment discharge: A flume based investigation,” in *The 12th International*
429 *Conference of International Association for Computer Methods and Advances in Geomechanics*
430 *(IACMAG)*, Goa, India, 2008. [Online]. Available: [ir.canterbury.ac.nz/bitstream/10092/
431 3134/1/12612367_Paper-IACMAG2008.pdf](http://ir.canterbury.ac.nz/bitstream/10092/3134/1/12612367_Paper-IACMAG2008.pdf) .
- 432 [49] C. Bosco, D. de Rigo, T. Dijkstra, G. Sander, and J. Wasowski, “Multi-Scale robust
433 modelling of landslide susceptibility: Regional rapid assessment and catchment robust fuzzy
434 ensemble,” *IFIP Adv. Inf. Commun. Technol.*, vol. 413, pp. 321-335, 2013. doi: [10.1007/978-3-
435 642-41151-9_31](https://doi.org/10.1007/978-3-642-41151-9_31) .